Coil Design for Integration with GaN Hall-Effect Sensors

Marsic, V., Faramehr, S. & Igic, P

DOI 10.1109/WiPDAEurope55971.2022.9936109
Electronic ISBN:978-1-6654-8814-3
Print on Demand(PoD) ISBN:978-1-6654-8815-0

Publisher: IEEE

Coil Design for Integration with GaN Hall-Effect Sensors

***Abstract*— In this paper, we report on and compare coil designs for Gallium Nitride (GaN) smart power integration, where the power switch is monolithically integrated with Hall-effect sensor. A detailed geometry optimization study for a coil routed around a GaN Hall-effect magnetic sensor is presented for current monitoring applications. An electromagnetic 3-dimensional model examines the dimensions and configurations of the coil in a single or multiple turns for integration with a senseHEMT to galvanically monitor the current of the main power switch. Using concentric receiving zones on the sensor surface, the theoretical results demonstrate how coil designs affect the magnetic field spatial distribution. We use the MATLAB environment as an extensively adopted computing platform to electromagnetically simulate priory design the coils for GaN smart power integration.**

Keywords—FEA, FEM, simulation, MATLAB, GaN, Hall

I. Introduction

Increasing efficiency, power density, and operating temperature range are all critical aspects of today's power electronic applications. Therefore, discrete devices based on GaN [1, 2] have been proliferating the power electronics industry. With higher power densities and efficiency than silicon counterparts [3], GaN power transistors possessing high electron mobility are now becoming cost-effective solutions on silicon substrates [4]. Mirroring the silicon technology evolution from discrete transistors to smart power integration circuits, the GaN based power transistors need to follow the same path for the widespread adoption of the technology in high volume applications.

For power electronics applications, a fast and accurate on-chip current monitoring is fundamental to facilitate control design, enhance system reliability and lifetime. Traditional current monitoring methods are based on shunt resistor measurements [5]. Recently, researchers at Fraunhofer Institute for Applied Solid State Physics demonstrated a shunt resistor technique for GaN high electron mobility transistors (HEMTs) [6]. Although purposeful, the shunt technique is not optimal for converters with 99% efficiency at frequencies higher than 65 kHz [7] and lacks galvanic isolation. Current monitoring through magnetic field offers the benefit of galvanic isolation from the power switch, however, it requires a magnetic sensor in close proximity to the conductor carrying a small portion of the current from main power switch through a senseHEMT. Fig. 1 illustrates an application where a Hall sensor detects the current flowing through a conductor shaped as a square coil for galvanic monitoring, while Fig. 2 represents the cross section of the GaN Hall-effect sensor integrated with the coil.

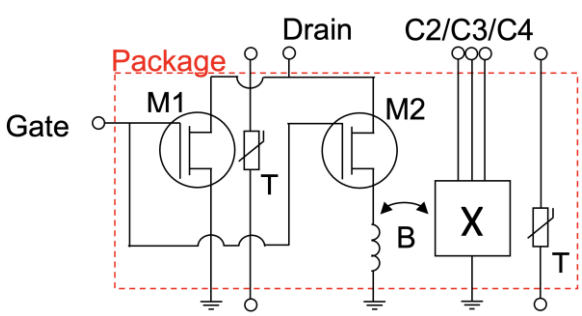

Figure 1. GaN smart power integrated circuit technology composed of a main power switch (M1), sesneHEMT (M2), coil and Hall-effect magnetic sensor.

Recent research developments in magnetic field sensing and spatial integration at PCB [8] and chip levels [9] have enabled the anticipated isolation provided by the Hall effect sensor from the power source to outperform the shunt measurement techniques. Nevertheless, the study of spatial dependence of a magnetic sensor exposed area with or without a material field concentrator for various shapes and geometries of the coil is a difficult, tedious, and slow task. Such a task requires training and access to expensive electromagnetic field solver software such as ANSYS Maxwell/HFSS [10], SIMULIA CST [11], or TCAD [12] for integration analysis at chip level or various time-consuming restrictive spaces experiments on PCB level components.

In this study, a 3-dimensional (3D) magnetic field analysis resulting from different coil configurations is presented at the edges of GaN Hall-effect sensor active regions. As this study uses the finite element method (FEM) integrated into MATLAB's electromagnetic toolbox, the analysis' accessibility will be extended to the wide user domain rather than to specialised isolated areas. Through an innovative simulation, finite element analysis (FEA) demonstrates the possibility of optimising sensor performance through 3D spatial manipulation, while utilising a single main parameter such as the incident magnetic flux intensity (B) on the sensor area. To the current author's knowledge, no previous study has reported similar simulations to optimise coil designs for GaN smart power integration.

One of the main outputs of this work is the 3D geometrical analysis and optimisation of coils for smart power integration at the pre-manufacturing stage. Furthermore, the innovative magneto-static FEA's methodology and results provide powerful insights into the spatial distribution of the magnetic field intensity at sensor active region prior to fabrication stage.

In the present system, the current is galvanically monitored with a GaN Hall-effect sensor [9, 13, 14] that will be monolithically integrated with a normally-off GaN power switch. The initial step toward demonstrating a smart power integrated circuit is the coil design.

II. Methodology

Through a preliminary 3D electromagnetic analysis, this study provides a methodology for optimising functionality of GaN Hall effect magnetic sensors in monolithic integration with a GaN power switch by investigating various coil designs. Additionally, the 3D analysis will be conducted with MATLAB's FEM solver, which is one of the most advanced tools that comes with default toolboxes capable to deliver electrostatic, magneto-static and harmonic simulations.

The simulation scenario is following the internal layered structure of the Hall sensor shown in Fig. 2. Fig. 3 illustrates the dimensions of the sensor used for FEM modelling, along with its electronic equivalent schematics (Fig. 3A) and the surface triangulation of the mesh elements (Fig. 3 C-D). The

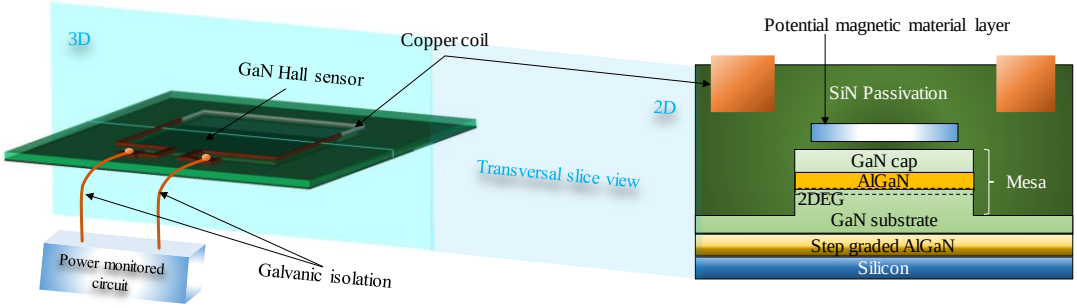

Figure 2. Hall sensor integrated in GaN technology: 3D and 2D structural architecture

3D simulation elements are initially designed in computer-aided design (CAD) software FreeCAD and imported into MATLAB as STL objects, then re-meshed using the partial differential equation (PDE) toolbox.

Real-life electronic circuits need to be powered by an external source, which is symbolically represented as a voltage or current source in schematics. Although the power sources close the positive and negative conductive paths in a continues loop, in simulations the power source implementation implies a mesh merger of the two separate paths, along with specifying in which node, edge or element an excitation field variable is located. Since it has already been shown that an omnidirectional source model can produce different results depending on its initial distribution pattern of the points [15], a higher degree of caution needs to be exercised when selecting an excitation for the simulation. Consequently, the simulation representation for the loop elements is a closed path with the excitation source being a uniform current density manifested at the vertices level and resulted from a 1V electric field amplitude on a copper conductivity of 59.6×106 Siemens/m.

Through our proposed computational study, we will use two loop configurations: one with a single turn whose width increases in 1 µm steps, and another with up to four turns. Each of the multi-turn loops maintains a constant width of 1 µm and a space of 0.5 µm between turns. The configurations are tested with and without a magnetic material between them, resulting in a total of 18 individual computational tests, as shown in Fig. 4.

The eighteen modelling configurations are centred around the Hall's square sensing volume of $10 \times 10 \times 0.06$ µm^3 placed 0.6 µm below the rectangular profile loop. The difference between half of the loop configurations and the other half is the presence or absence of a magnetic film with volume of $9 \times 9 \times 0.2$ µm^3 assigned with a relative permeability of 1000 (i.e., corresponding to the CoTaZr alloy [16]).

The interest reception region is the area located between the top surface of the Hall sensor and the bottom surface of the magnetic layer. The area is divided into five distinct concentric zones proportional with the 1 µm width and height of the multi-turn loops or width extension rate of 1 µm for single-turn loops. Fig. 5 illustrates a geometrical relationship between the magnetic field lines surrounding the loop conductor and the Hall sensor's receiving area divided into distinct zones. Each measurement zone contains a distinct number of Cartesian grid points on which the magnetic flux components have been interpolated, averaged, and summed. By averaging the scalar result B, we aim to provide an

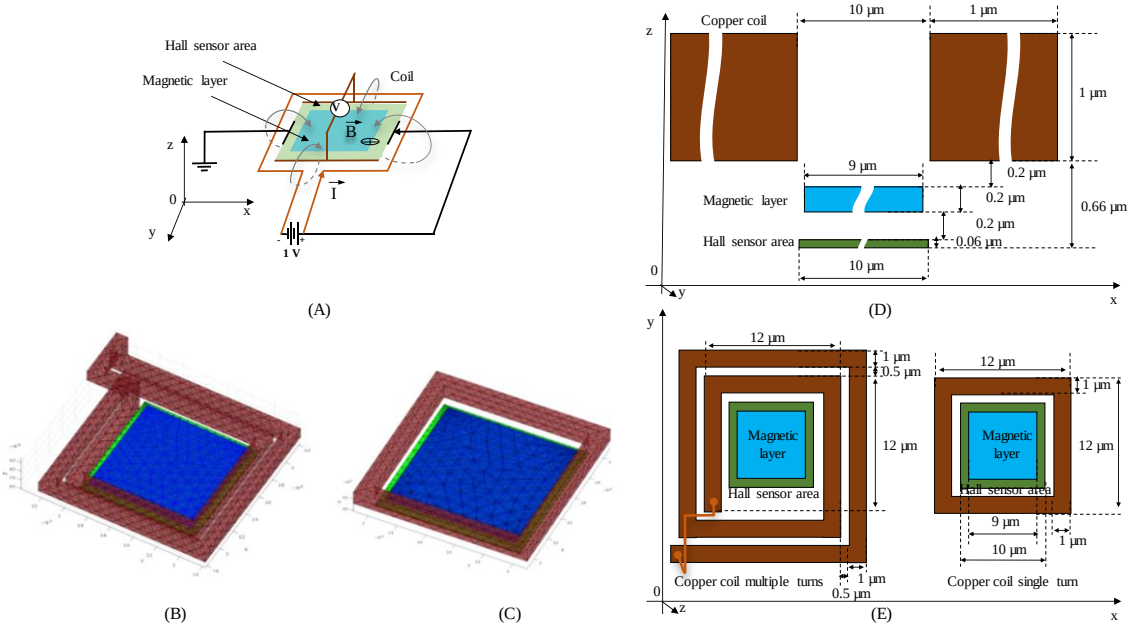

Figure 3. Hall sensor for FEM simulation scenario (dimensions not at scale): Simulation scenario electrical equivalent circuit (A); FEM simulation mesh for a two turns coil (B); FEM simulation mesh for a single turn coil (C); FEM simulation scenario, side view and dimensions (D); FEM simulation scenario, top view and dimensions (E)

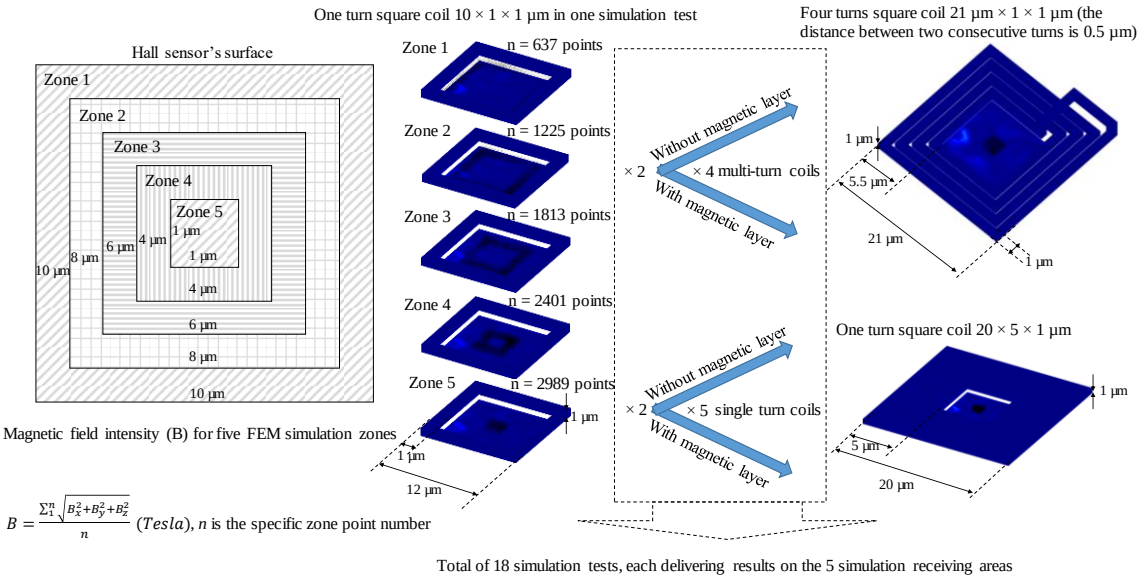

Figure 4. Hall sensor FEM simulation areas distribution for investigation and brief details of the successive simulation scenarios characteristics

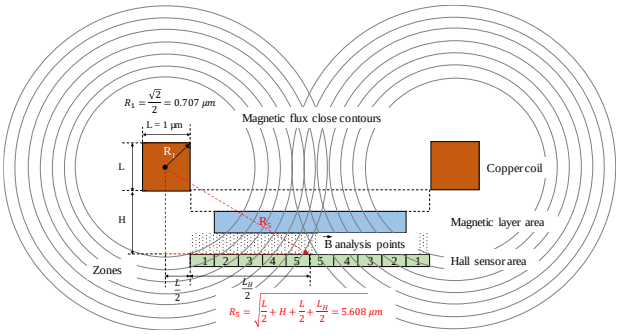

Figure 5. Hall sensor area divided in the simulation measuring zones and potential relationship established between loop's magnetic field

introspective view of the overall complex interactions at the field-material level, while abstracting the potential isolated simulation errors resulting from series expansion truncation in solvers, discretization errors resulted in large simulation scenarios or round-off computational errors. The whole simulation scenario was placed in a virtual air test box enclosure (i.e., not shown in the images), as required in FEM computation, and the relative permeability for air, copper, and Hall sensor areas was 1, 0.99, and 0.99, respectively.

III. Results and Discussion

As shown in Fig. 6, the four graphs plot the results of 18 simulation tests on five different receiving zones. When the magnetic layer is present, the averaged magnetic flux intensity varies between 200 µT to 1500 µT, and from 2 µT to 27 µT

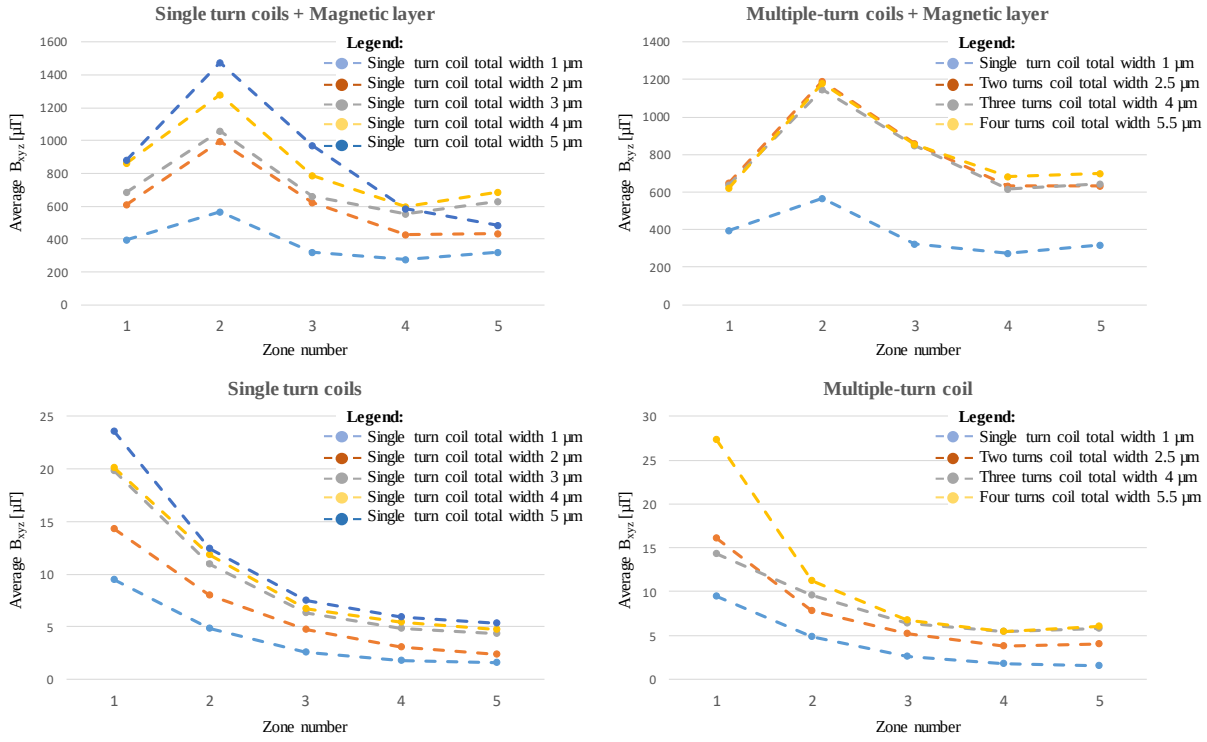

Figure 6. MATLAB FEM simulation results plotted for the average value of the magnetic field B on each of the five investigated receiving areas

when absent. The results confirm the acknowledged fact that several orders of magnitude of improvement can be achieved with a magnetic material placed between a coil and the Hall effect magnetic sensor. However, contrary to the popular belief that the central area (i.e., zone 5) will exhibit the highest magnetic field value due to the spatial density concentration of the field lines, the area closest to the loop exhibits the highest intensity, as for all electromagnetic radiation sources. For the scenarios with the magnetic layer, the highest values occur in zone two, which is closest to the magnetic layer surface and the loop, as the magnetic material area is a square of 9×9 μm^2, 1 μm shorter when compared to the sensor's receiving area of 10×10 μm^2.

Another observation can be made on the differences between loops covering similar areas that involve multiple turns and loops with single turns. Consequently, the three multi-turn loop results are similar to the single-turn loop with a width of 4 μm. The result is consistent with electromagnetic modelling, which considers multi-turn loops as a single volume instead of implementing successive spiralled layers. Both structural arrangements offer individual advantages in specific designs where conductive area, operation frequencies, and proximity to other electronic components need to be considered. The overall results suggest that a wider loop with a magnetic material layer can produce the highest magnetic field values on the Hall sensor surface, simplifying complicated arrangements and geometries involving multi-turn loops.

IV. Conclusions and Further Work

The 3D FEA simulations of coil designs for a GaN smart power integration was successfully demonstrated using MATLAB. The simulation results support the initial hypothesis that sensor sensitivity can be increased through priory manufacturing spatial optimization. The 4 μm wide single-turn coil has demonstrated trough comparison in both with and without the magnetic layer that less complexity could reduce the intricate path routing analysis and implicit errors.

A future study will focus on the magnetic field's incidence angle on receiving area in order to complete the picture of the sensing-positioning optimisation process, since the current study only accounted for the magnetic field intensity. This study provides a design demonstration that may provide the basis for future efficient sensor integration whereas the 3D simulation approach in MATLAB serves as an example of electromagnetic analysis across a broad spectrum of users.

References

[1] S. Faramehr and P. Igić, "Analysis of gan hemts switching transients using compact model," *IEEE Transactions on Electron Devices,* vol. 64, no. 7, pp. 2900-2905, 2017.

[2] B. Ubochi, S. Faramehr, K. Ahmeda, P. Igić and K. Kalna, "Operational frequency degradation induced trapping in scaled GaN HEMTs," *Microelectronics Reliability* , vol. 71, pp. 35-40, 2017.

[3] H. Amano, Y. Baines, E. Beam, M. Borga, T. Bouchet, P. R. Chalker, M. Charles, K. Chen, N. Chowdhury, R. Chu and C. De Santi, "The 2018 GaN power electronics roadmap," *Journal of Physics D: Applied Physics,* vol. 51, no. 16, p. 163001, 2018.

[4] T. Ueda, "GaN power devices: Current status and future challenges," *Japanese Journal of Applied Physics,* vol. 58, no. SC, p. SC0804, 2019.

[5] W. Pribyl, "Integrated smart power circuits technology, design and application," in *Proceedings of the 22nd European Solid-State Circuits Conference*, 1996.

[6] S. Moench, R. Reiner, P. Waltereit, R. Quay, O. Ambacher and I. Kallfass, "Integrated current sensing in GaN power ICs," in *31st International Symposium on Power Semiconductor Devices and ICs (ISPSD)*, 2019.

[7] S. Moench, R. Reiner, P. Waltereit, J. Hueckelheim, D. Meder, R. Quay, O. Ambacher and I. Kallfass, "A 600v gan-on-si power ic with integrated gate driver, freewheeling diode, temperature and current sensors and auxiliary devices," in *11th International Conference on Integrated Power Electronics Systems (CIPS)*, 2020.

[8] M. Kashmiri, "Current sensing techniques: Principles and readouts," in *Next-Generation ADCs, HiPerformance Power Management, and Technology Considerations for Advanced Integrated Circuits*, Springer Cham, 2020, pp. 143-165.

[9] S. Faramehr, N. Poluri, P. Igić, N. Janković and M. M. D. Souza, "Development of GaN Transducer and On-Chip Concentrator for Galvanic Current Sensing," *IEEE Transactions on Electron Devices,* vol. 66, no. 10, pp. 4367-4372, 2019.

[10] V. Sangwan, D. Kapoor, C. M. Tan, C. H. Lin and H.-C. Chiu, "High-frequency electromagnetic simulation and optimization for GaN-HEMT power amplifier IC," *IEEE Transactions on Electromagnetic Compatibility,* vol. 61, no. 2, pp. 564-571, 2018.

[11] B. J. Alex and T. Beechner, "GaN module design recommendations based on the analysis of a commercial 3-phase GaN module," in *IEEE Energy Conversion Congress and Exposition (ECCE)*, 2019.

[12] S. Faramehr, N. Janković and P. Igić, "Analysis of GaN MagHEMTs. 33, no. 9 (2018," *Semiconductor Science and Technology,* vol. 33, no. 9, p. 095015, 2018.

[13] P. Igic, N. Jankovic, J. Evans, M. Elwin, S. Batcup and S. Faramehr, "Dual-drain GaN magnetic sensor compatible with GaN RF power technology," *IEEE Electron Device Letters,* vol. 39, no. 5, pp. 746-748, 2018.

[14] B. R. Thomas, S. Faramehr, D. C. Moody, J. E. Evans, M. P. Elwin and P. Igić, "Study of GaN dual-drain magnetic sensor performance at elevated temperatures," *IEEE Transactions on Electron Devices,* vol. 66, no. 4, pp. 1937-1941, 2019.

[15] V. Marsic, E. Kampert and M. D. Higgins, "Ray Tracing 3D Source Modelling for Optical Reflectance Sensing with Wireless Ranging Application," in *IEEE International Symposium on Robotic and Sensors Environments (ROSE)*, 2021.

[16] D. S. Gardner, G. Schrom, P. Hazucha, F. Paillet, T. Karnik, S. Borkar, J. Saulters, J. Owens and J. Wetzel, "Integrated on-chip inductors with magnetic films," in *IEEE International Electron Devices Meeting*, 2006.